OPTIMUM DESIGN OF 3R ORTHOGONAL MANIPULATORS CONSIDERING ITS TOPOLOGY

Giovana Trindade da Silva Oliveira, gtrindadeso@yahoo.com.br
School of Mechanical Engineering, Federal University of Uberlândia, 2160 João Naves de Ávila Av., Campus Santa Mônica, CEP 38400-902, Uberlândia, Brazil.

Antônio Carlos Nogueira, anogueira@ufu.br
Sezimária Fátima Pereira Saramago, saramago@ufu.br
College of Mathematics, Federal University of Uberlândia, 2160 João Naves de Ávila Av., Campus Santa Mônica, CEP 38400-902, Uberlândia, Brazil.

Abstract. *Several studies have investigated the properties of the workspace open chains robotics with the purpose of emphasizing its geometric and kinematic characteristics, and to devise analytical algorithms and procedures for its design. The workspace of a manipulator robot is considered of great interest from theoretical and practical viewpoint. The workspace topology is defined by the number of kinematic solutions, the number of cusps and nodes that appear on the workspace boundary. In the classic applications in the industry, manipulators need to pass through singularities of the joint space to change their posture. A 3-revolute (3R) manipulator can execute a non singular change of posture if and only if there is at least one point in its workspace which has exactly three coincident solutions of the inverse kinematic model. In this work, a mulit-objective optimization problem is formulated with the aim of obtaining the optimal geometric parameters of robot which must obey the topology specified by the designer. The maximum workspace volume, the maximum system stiffness and the optimum dexterity are considered as the multi-objective functions. In addition, the optimization problem is subject to penalties that control the topology, forcing it to occupy a certain portion of the workspace. A sequential technique and evolutions algorithms are applied in the solution of the problem. Some applications are presented to show the efficiency of the proposed methodology.*

Keywords*: robotics, manipulators topology, optimization, workspace volume, robot stiffness, robot dexterity.*

1. INTRODUCTION

In the classic applications in the industry, manipulator robots need to pass through singularities of the joint space to change their posture. A 3-revolute (3R) manipulator can execute a non singular change of posture if and only if there is at least one point in its workspace which has exactly three coincident solutions of the inverse kinematic model (IKM), resulting in one of the separation surface which divide the workspace in several regions that have manipulators with same properties (binary or quaternary, regions with the same numbers of cusps and node points). These regions are called domains. So, to study such manipulators is essential to know the topology of the singularity surfaces in the workspace. These singularities are defined as places where the determinant of the Jacobian matrix of direct kinematic model (DKM) is annulled, defining the others equations of surfaces which divide the workspace.

Wenger and El Omri (1996) showed that for some choices of the parameters, manipulators with three rotational joints (3R) may be able to change posture without meeting a singularity in the joint space. They succeed in characterizing such manipulators (Wenger, 1998), but they needed general conditions on the design parameters. Corvez (2002) found important results about this issue. In 2004, Baili realized researches on the proprieties of 3R manipulators with orthogonal axes and made a classification in the parameters space.

Oliveira *et al*. (2009) showed a separation surfaces formulation by using the algebraic tool Grobner basis to obtain an analytical expression of the surfaces of the parameters space that separate the different types of manipulators. The other surfaces were obtained by annulment of the determinant of Jacobian matrix of the direct kinematic model.

In this paper, a multi-objective optimization problem is formulated with the aim of obtaining the optimal geometric parameters of robot which must obey the topology specified by the designer. The maximum workspace volume, the maximum system stiffness and the optimum dexterity (expressed with condition number of Jacobian matrix) are considered as multi-objective function.

This paper also discusses a comparative study of three different numerical techniques, i.e., sequential quadratic programming (SQP), genetic algorithms (GA) and differential evolution (DE). The presence of voids and singularities and the discontinuous generation of the envelope greatly increase the complexity of the calculation of the algebraic formulation for a correct mathematical model of the robot. Moreover, the objective function presents several local maxima and is extremely nonlinear. These factors greatly increase the difficulties involved in the optimization process, justifying the use of different optimization techniques to validate the results. It is known that conventional methods are based on a rule of point-to-point and has the danger of falling into local optima.

The evolutionary algorithms are based on the population-to-population rule. These techniques have the advantages of robustness and good convergence properties. They require no knowledge or gradient information about the optimization problems, in this case only the objective function and corresponding fitness levels influence the directions

of search. The discontinuities present on the optimization problems have little effect on the overall optimization performance. The probabilistic transition rules are used and they perform well for large-scale optimization problems in the presence of local optima. In this work two evolutions algorithms are applied in the solution of the problem: Genetic Algorithms (GA) and Differential Evolution (DE). GA and DE have been shown efficient to solve linear and nonlinear problems by exploring all regions of search space and exponentially exploiting promising areas through mutation, crossover, and selection operations applied to individuals in the population. Therefore, they are the suitable for the optimization problems studied here.

The manipulators with three rotational joints with orthogonal axes as described in Fig. 1. The study of this type of manipulator is done according to the Denavit-Hartenberg parameters: d_2, d_3, d_4, r_2, and r_3. To reduce the number of parameters, will be considered $d_2 = 1$ and $r_3 = 0$. The joint variables are θ_1, θ_2 and θ_3 which represent the input angles of the actuators. For this type of manipulator, the direct kinematic model is given in Eq. (1):

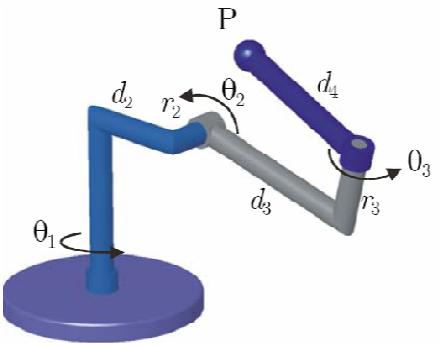

Figure 1. Manipulator with three rotational joints (3R) with orthogonal axes

$$\begin{aligned} x &= \left[1+\left(d_3+d_4c\theta_3\right)c\theta_2\right]c\theta_1-\left(r_2+d_4s\theta_3\right)s\theta_1 \\ y &= \left[1+\left(d_3+d_4c\theta_3\right)c\theta_2\right]s\theta_1+\left(r_2+d_4s\theta_3\right)c\theta_1 \\ z &= -\left(d_3+d_4c\theta_3\right)s\theta_2 \end{aligned} \tag{1}$$

in which $c_i = \cos\theta_i$ and $s_i = \sin\theta_i$, for $i = 1, 2, 3$.

A powerful algebraic tool is used: the Grobner basis. With this approach, it is possible to obtain analytical expressions of the surfaces of the parameters space that separate the different types of manipulators. The annulment of the determinant of Jacobian matrix of the inverse kinematic model (IKM) enables to obtain the other surfaces that separate the various regions for different topologies (Oliveira *et al*, 2009). Thus, it is possible obtain:

$$C_1 : d_4 = \sqrt{\frac{1}{2}\left(d_3^2+r_2^2-\frac{\left(d_3^2+r_2^2\right)^2-d_3^2+r_2^2}{AB}\right)}, \text{ where } A=\sqrt{(d_3+1)^2+r_2^2} \text{ and } B=\sqrt{(d_3-1)^2+r_2^2} \tag{2}$$

The Equation (2) is the surface of separation between the manipulators of domain 1 and domain 2. The manipulators that belong to domain 1 are binary, have a toroidal cavity in its workspace and do not have cusps and nodes points. The domain 2 represents the manipulators that have 4 points of cusp, but do not have the same number of nodes.

The surface of separation C_2 between the domains 2 and 3 is defined by:

$$C_2 : d_4 = d_3/(1+d_3).\sqrt{(d_3+1)^2+r_2^2} \tag{3}$$

The domain 3 is composed by manipulators which present 2 cusps points on internal envelopment. In the case of domain 4, the manipulators have 4 points of cusp and 4 nodes. The surface C_3, which separates the manipulators of the domains 3 and 4, is given by:

$$C_3 : d_4 = d_3/(d_3-1).\sqrt{(d_3-1)^2+r_2^2}, \text{ with } d_3 > 1 \tag{4}$$

Finally, the domain 5 corresponds to manipulators that have no cusp points. Unlike of manipulators of the type 1, the internal envelope is not defined by a toroidal cavity, but by a region with 4 solutions in IKM. The surface of separation C_4 between the domains 3 and 5 is:

$$C_4 : d_4 = d_3/(1-d_3).\sqrt{(d_3-1)^2+r_2^2}, \text{ with } d_3 < 1 \tag{5}$$

Summarizing, the space of parameters (d_3, d_4 and r_2) of a 3R orthogonal manipulator is divided into 5 domains separated by surfaces C_1, C_2, C_3 and C_4, defined by Eqs. (2), (3), (4) and (5), respectively.

The Figure 2a) shows the curves of separation in a plane section (d_3, d_4) of the space of parameters, resulting in 5 domains, adopting a fixed value for r_2 =1. The Figure 2b) shows the space of parameters divided according to the number of cusps points and nodes points. The domains according to the number of cusps points are divided into sub-domains that contain the same number of nodes. Each sub-domain defines a topology of the workspace denoted $WT_i(\alpha, \beta)$, where α represents the number of cusp points and β the number of nodes points.

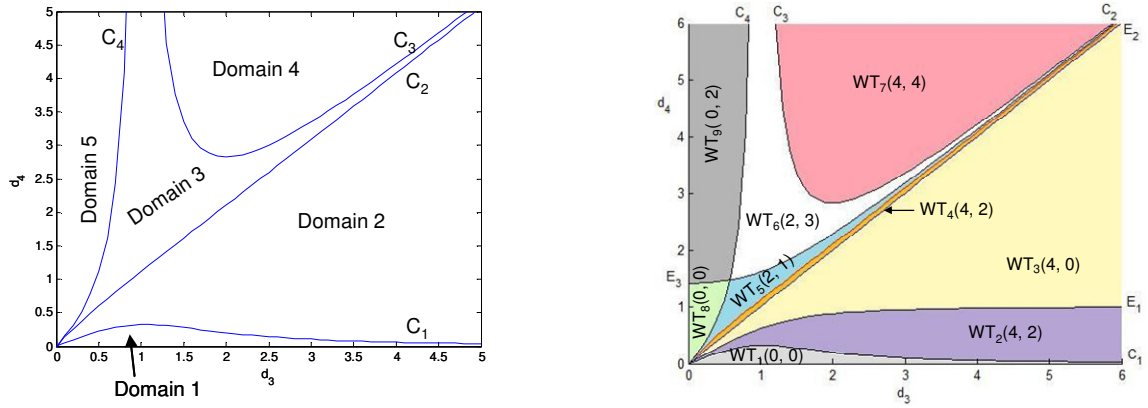

(a) (b)

Figure 2. Division of parameters space considering r_2 = 1:
(a) According to the surface of separation of topologies; (b) According to the number of points of cusps and nodes

As explained previously, the manipulators of the domain 1 have a toroidal cavity and do not have cusps and nodes points. The manipulator represented in Fig. 3a) characterize the first type of manipulator, whose topology is known as $WT_1(0, 0)$.

The manipulators that belong to domain 2 have 4 points of cusp. This region can be subdivided into 3 sub-domains through the surfaces E_1 and E_2. The topology of the workspace $WT_2(4, 2)$, represented by Fig. 3b), has 4 cusp points, 2 nodes, a toroidal cavity, two regions with 4 solutions and a region with 2 solutions in IKM. The topology $WT_3(4, 0)$ contains manipulators with 4 cusp points, zero node, without toroidal cavity, a region with 4 solutions and other with 2 solutions in IKM, as illustrated in Fig. 3c). The transition between the topologies WT_2 and WT_3 is the boundary between the manipulators containing a toroidal cavity in its workspace and those that do not contain. According to Baili (2004), the surface of separation between these topologies is given by the expression:

$$E_1 : d_4 = 0.5\,(A - B), \text{ where } A \text{ and } B \text{ are given in Eq. (2).} \tag{6}$$

In domain 2 is still possible to characterize the topology represented in the Fig. 4d), denoted by $WT_4(4, 2)$, containing 4 points of cusp and 2 nodes. These nodes are different from nodes of WT_2 since not delimit a toroidal cavity but a region of 4 solutions in IKM. In this case, the surface of separation E_2, between topology WT_3 and WT_4 is defined by:

$$E_2 : d_4 = d_3 \tag{7}$$

The domain 3 is composed by manipulators which have 2 cusp points and can be divided into 2 sub-domains through the surface E_3. The manipulators described by $WT_5(2, 1)$ have 2 cusps points on internal envelope, a node point and has the shape of a fish, as shown Fig. 3e). Moreover, the Fig. 5f) presents a manipulator that belongs to the workspace $WT_6(2, 3)$, which has 2 points of cusp and 3 nodes. The Eq. (8) defines the separation surface between the topology WT_5 and WT_6. Besides, this surface also separates the topology of the workspace WT_8 and WT_9 that are contained in the domain 5.

$$E_3 : d_4 = 0.5\,(A + B) \tag{8}$$

In domain 4, the manipulators are of type 4, represented by $WT_7(4, 4)$, have 4 cusp points and 4 nodes, as can be seen in Fig. 3g). The 4 points of cusp are shared between the internal and external singularity surfaces.

Finally, the domain 5 corresponds to manipulators that have no cusp points. Unlike of manipulators of the type 1, the internal envelopment is not defined by a toroidal cavity, but by a region with 4 solutions in IKM.

The domain 5 corresponds to manipulators of type 5 and do not have cusp points. This region is divided into 2 sub-domains through the surface E_3. In the Fig. 3h), the topology represented by WT_8 (0, 0) does not have cusp points and nor nodes. As mentioned earlier, its internal envelope is not defined by a toroidal cavity, but by a region with 4

solutions in IKM. Finally, Fig. 3i) features a manipulator which belongs to the topology WT_9 (0, 2), with 0 cusp points and 2 nodes points obtained by the intersection of internal and external envelopment.

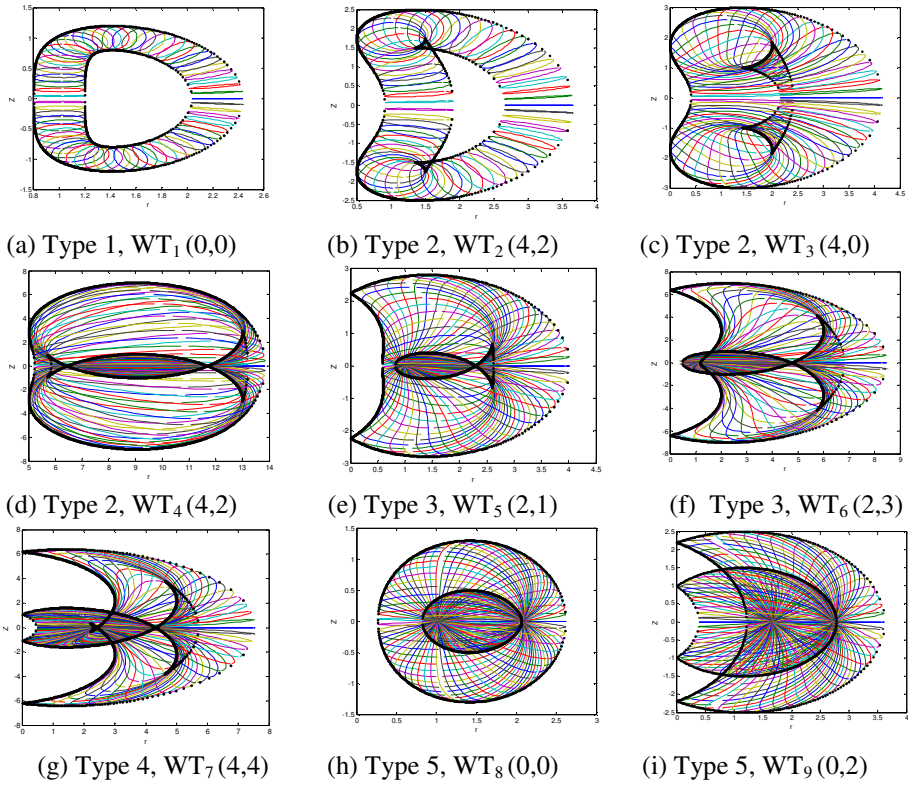

(a) Type 1, WT_1 (0,0) (b) Type 2, WT_2 (4,2) (c) Type 2, WT_3 (4,0)

(d) Type 2, WT_4 (4,2) (e) Type 3, WT_5 (2,1) (f) Type 3, WT_6 (2,3)

(g) Type 4, WT_7 (4,4) (h) Type 5, WT_8 (0,0) (i) Type 5, WT_9 (0,2)

Figure 3. Radial section for 3R orthogonal manipulator, showing the 5 types of manipulators

2. WORKSPACE OF 3R MANIPULATORS

According to Bergamaschi *et al* (2006), the workspace W is the set of all attainable points for a point P of the end-effector when the joint variables sweep its definition interval entire. Point P is usually chosen as the center of the end-effector, or the tip of a finger, or even the end of the manipulator itself. The first procedure to investigate the workspace is to vary the angles θ_1, θ_2 and θ_3 in their interval of definition and to estimate the coordinates of point P with respect to the manipulator base frame. The workspace of this robot is a solid of revolution. Thus, it is natural to imagine that the workspace is the result of rotation around the z axis of a radial plane section.

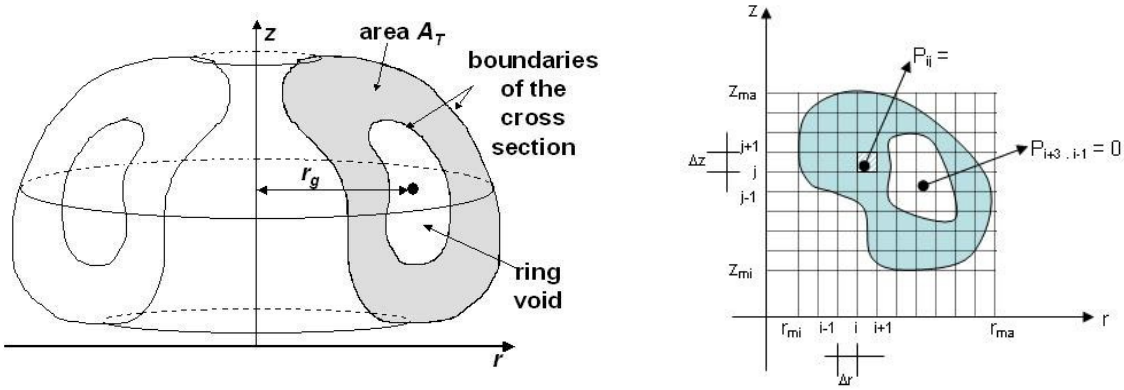

Figure 4. (a) A scheme for evaluating the workspace volume of 3R manipulators; (b) Discretization of cross section area by using a rectangular mesh

The workspace of a three-revolute open chain manipulator can be given in the form of the radial reach r and axial reach z with respect to the base frame, according to Bergamaschi *et al*. (2006). For this representation, r is the radial distance of a generic workspace point from the z-axis, and z is the distance of this same point at the XY-plane (see Fig. 4b). Thus, using Eq. (1), the parametric equations (of parameters θ_2 and θ_3) of the geometrical locus described by

point *P* on a radial plane are:

$r^2=x^2+y^2$ and z, where x, y and z are given in (1). (9)

The workspace volume *V* can be evaluated by the Pappus-Guldin Theorem, using the following equation (see Fig. 4a):

$V = 2\pi r_g A_r$, where A_r is the cross section area, which is formed by the family of curves given by Eq. (1). (10)

This research proposes numerical formulation to approximate the cross section area, through its discretization within a rectangular mesh. Initially, the extreme values of vectors *r* and *z* should be obtained as:

$$r_{min} = \min\{r\}, \quad r_{max} = \max\{r\}, \quad z_{min} = \min\{z\} \quad \text{and} \quad z_{max} = \max\{z\} \tag{11}$$

Adopting n_r and n_z as the number of intervals chosen for the discretization along the *r* and *z* axis, the sizes of the elementary areas of the mesh can be calculated:

$$\Delta r = (r_{\max} - r_{\min})/n_r \quad \text{and} \quad \Delta z = (z_{\max} - z_{\min})/n_z \tag{12}$$

The n_r and n_z values must be adopted so that the sizes of the elementary areas (Δr or Δz) are at least 1% of the total distances considered in the discretization ($r_{\max}$ - $r_{\min}$ or $z_{\max}$ - $z_{\min}$). Every point of the family of curves form the cross section of the workspace is calculated by Eq. (9). Using this equation, varying the values of θ_2 and θ_3 in the interval $[-\pi, \pi]$, it is possible to obtain the family of curves of the workspace. Given a certain point (r, z), its position inside the discretization mesh is determined through the following index control:

$$i = \text{int}[(r - r_{\min})/\Delta r] + 1 \quad \text{and} \quad j = \text{int}[(z - z_{\min})/\Delta z] + 1 \tag{13}$$

where i and j are computed as integer numbers. As shown in Fig. 5b), the point of the mesh that belongs to the workspace is identified by $P_{ij} = 1$, otherwise $P_{ij} = 0$, which means:

$P_{ij} = 0$, if $P_{ij} \notin W(P)$ *or* 1, *if* $P_{ij} \in W(P)$; where $W(P)$ indicates workspace region. (14)

In this way, the total area is obtained by the sum of every elementary areas of the mesh that are totally or partially contained in the cross section. In Eq. (14), it is observed that only the points that belong to the workspace contribute to the calculation of the area A_T. The coordinate r_g of the center of the mass is calculated considering the sum of the center of the mass of each elementary area, divided by the total area, using the following equation:

$$A_T = \sum_{i=1}^{i_{\max}} \sum_{j=1}^{j_{\max}} \left(P_{ij}\, \Delta r\, \Delta z\right) \quad \text{and} \quad r_g = \left(\sum_{i=1}^{i_{\max}} \sum_{j=1}^{j_{\max}} \left(P_{ij}\, \Delta r\, \Delta z\right)\left((i-1)\, \Delta r + (\Delta r/2) + r_{\min}\right) \right) / A_T \tag{15}$$

Finally, after the calculation of the cross section area and the coordinate of the center of the mass, given by Eqs. (14) and (15), respectively, the workspace volume of the manipulator can be evaluated by using Eq. (10).

3. SYSTEM STIFFNESS

From the viewpoint of mechanics, the stiffness is the measurement of the ability of a body or structure to resist deformation due to the action of external forces. The stiffness of a serial mechanism at a given point of its workspace can be characterized by its stiffness matrix. This matrix relates the forces and torques applied at the gripper link in Cartesian space to the corresponding linear and angular Cartesian displacements.

Two main methods have been used to establish mechanism stiffness models. The first one is called matrix structural analysis, which models structures as a combination of elements and nodes. The second method relies on the calculation of the serial mechanism's Jacobian matrix which is adopted in this work.

Matrix *J* is usually termed Jacobian matrix which is described in Eq. (16). By considering the case in that d_2=1, its determinant is calculated by using the Eq. (17).

$$[J]=\begin{pmatrix} -\sin\theta_3\cos\theta_2 d_4-\cos\theta_2 r_2 & 0 & -\sin\theta_3 d_4 \\ \sin\theta_3\sin\theta_2 d_4+\sin\theta_2 r_2 & d_3+\cos\theta_3 d_4 & 0 \\ \cos\theta_2 d_3+\cos\theta_2\cos\theta_3 d_4+d_2 & 0 & \cos\theta_3 d_4 \end{pmatrix} \tag{16}$$

$$\det(J)=d_4\left(d_3+d_4\cos\theta_3\right)\left[d_2\sin\theta_3+\left(d_3\sin\theta_3+\left(d_3\sin\theta_3-r_2\cos\theta_3\right)\cos\theta_2\right)\right] \tag{17}$$

The stiffness matrix of the mechanism in the Cartesian space is then given by the Eq. (18), where K_j is the joint stiffness matrix of the mechanism, with $K_j=[k_1, k_2, k_3]$. In this case, each actuators of the mechanism is modeled as an elastic component. k_i is a scalar representing the joint stiffness of each actuator, which is modeled as linear spring:

$$K_C=[J]^T K_j[J] \tag{18}$$

Particularly, in the case for which all the actuators have the same stiffness, i.e., $k=k_1=k_2=k_3$, then Eq. (18) will be reduced to:

$$K_C=k[J]^T[J] \tag{19}$$

Furthermore, the diagonal elements of the stiffness matrix are used as the system stiffness value. These elements represent the pure stiffness in each direction, and they reflect the rigidity of machine tools more clearly and directly. The objective function for system stiffness optimization can be written as Eq. (20). In this case, the stiffness index S can be maximized:

$$S=K_{11}+K_{22}+K_{33} \tag{20}$$

4. DEXTERITY

The condition number of the Jacobian matrix will be used as a measure of dexterity indices for the 3R manipulator. By using the spectral norm, these indices will be described as.

$$Cond(J)=|\lambda_{\max}(J)/\lambda_{\min}(J)| \tag{21}$$

where $\lambda_{\max}$ and $\lambda_{\min}$ means the maximum and minimum singular values of Jacobian matrix J, respectively. Regarding the computing time of optimization process, this expression is selected as the objective function for the optimization of dexterity. The value of $Cond(J)$, which is directly related to singular values of Jacobian matrix, is between 1 and positive infinity. All the singular values of the Jacobian matrix will be the same and the manipulator is isotropic if $Cond(J)$ is equal to 1. While $Cond(J)$ is prone to be positive infinity it means that the Jacobian matrix is singular. Therefore, for the optimization of dexterity, the condition number must to be minimized.

5. NUMERICAL SIMULATIONS

The optimization problem is formulated with the objective of obtaining the optimal geometric parameters of the 3R manipulator to maximize the workspace and the system stiffness and to optimize the dexterity such as the topologies specified by the designer are obeyed. Since the problem have several objectives, it deals with a multi-objective optimization problem, it is required to find all possible tradeoffs among multiple objective functions that are usually conflicting with each other. The constraints depend on the topology chosen for the robot, according to Fig. 3. In this work, the optimization is investigated using a Sequential Quadratic Programming (SQP), the Differential Evolution (DE) and Genetic Algorithms (AG).

The evolutionary algorithms were developed for unconstrained problems. So, in the case of constrained optimization problems, it is necessary to introduce modifications in this method. This work uses the concept of Penalty Function (Nocedal and Wright, 2000). In this technique, the problems with constrains are transformed in unconstrained problems adding a penalty function $P(x)$ to the original objective function to limit constraint violations. This new objective function is penalized, according to a factor r_p, every time that meets an active constraint. The scalar r_p is a multiplier that quantifies the magnitude of the penalty. For the efficiency of the evolutionary method, a large value of the penalty factor r_p should be used to ensure near satisfaction of all constraints, in this research, was adopted r_p=1000. Then, the problem can be rewrite as follows:

$$\text{Maximize } F(x)=f(x)+r_p P(x), \text{ where } f(x)=[V, Cond(J), S] \text{ and } P(x)=\max(0, g_j(x))^2 \tag{22}$$

$$\text{Subject to: } g_j(x)\le 0;\ j=1,..,k \text{ and } x^l\le x_i\le x^u,\ i=1, 2, 3$$

The geometric parameters are design variables given by $x = (d_3, d_4, r_2)^T$. The lower and upper bounds adopted for the arm length (side constraints) are: $0.1 \leq x_i \leq 3.0$, $i = 1,2,3$.

In this simulation, two methods of multi-objective optimization are utilized: Weighting Objectives Method and Global Criterion Method (L_{2r}-metric and L_{3r}-metric) presented on Oliveira and Saramago (2010).

The weighted sum strategy converts the multi-objective problem vector $f(x)$ into a scalar optimization problem by building a weighted sum of all the objectives as Eq. (23). The weighting coefficients w_i represent the relative importance of each criterion. Thus,

$$\text{Maximize } F(x) = w_1 Vc_1 - w_2 Cond(J)c_2 + w_3 Sc_3 - r_p P(x) \text{ , where } \sum_{i=1}^{3} w_i = 1 \tag{23}$$

where the workspace volume V is given by Eq. (10), the stiffness S is calculated using the Eq. (20) and the condition number $Cond(J)$ is represented in the Eq. (21).

Objective weighting is obviously the most usual substitute model for vector optimization problems. The trouble here is attaching weighting coefficients to each of the objectives. The weighting coefficients do not necessarily correspond directly to the relative importance of the objectives or allow trade-offs between the objectives to be expressed. For the numerical methods for seeking the optimum of (23) so that w_i can reflect closely the importance of objectives, all the functions should be expressed in units of approximately the same numerical values. The best results are usually obtained if $c_i = 1/f_i^o$, where f_i^o represents the ideal solution, that indicates the minimum value of each i-th function. To determine this solution, one must find the minimum attainable for all the objective functions separately. In this case, the vector $f^o = [V_{id}, S_{id}, Cond(J)_{id}]^T$ is ideal for a multi-objective optimization problem.

In Global Criterion Method, the multi-objective optimization problem is transformed into a scalar optimization problem by using a global criterion. The function that describes this global criterion must be defined such as a possible solution close to the ideal solution is found. In this case, the L_{2r}-metric and L_{3r}-metric, are given respectively by:

$$\text{Minimize } F(x) = \left(\left(\frac{V_{id} - V}{V_{id}} \right)^2 + \left(\frac{Cond(J)_{id} - Cond(J)}{Cond(J)_{id}} \right)^2 + \left(\frac{S_{id} - S}{S_{id}} \right)^2 \right)^{1/2} + r_p P(x) \tag{24}$$

$$\text{Minimize } F(x) = \left(\left| \frac{V_{id} - V}{V_{id}} \right|^3 + \left| \frac{Cond(J)_{id} - Cond(J)}{Cond(J)_{id}} \right|^3 + \left| \frac{S_{id} - S}{S_{id}} \right|^3 \right)^{1/3} + r_p P(x) \tag{25}$$

The computational code of the DE was developed in MATLAB® by the authors. The parameters used were: number of population individuals $Np = 15$; 100 generations, representation of individuals by real vectors using multiplier of the difference vector $F = 0.8$ and crossover probability $CR = 0.5$.

The Genetic Algorithms Optimization Toolbox (GAOT) program developed by Houck *et al*. (1985) has been used to perform the GA, adopting $Np = 80$ individuals, 100 generations, crossover and mutation probabilities: 0.60 and 0.02.

The Sequential Quadratic Programming (SQP) it was performed by using the toolbox *fmincon* of the MATLAB®.

5.1 Example 1 - WT_1(0, 0)

In Example 1 is considered an application where the manipulator must belong to the topology WT_1 (see Fig. 3). In this case, the following constraints are adopted:

Side limits: $0.1 < d_3 < 3.0$; $0.1 < d_4 < 3.0$ e $0.1 < r_2 < 3.0$ [u.l.] and (26)
Points below the curve C_1, given by Eq. (2).

The ideal solution calculated using DE is: V_{id}=315.298 [u.v.]; $Cond(J)_{id}$=1.517 and S_{id}=27.009 [u.s.].

It is worth noting that when SQP is applied the optimum depends on the initial estimate provided by the user. Thus, tests were performed for different initial values resulting in different answers. This behavior clearly indicates the presence of several local minima. Several starting points were tested: the upper and lower limits of the search space, the midpoint of the range and the optimal solution obtained by DE. In the results presented in the Tab. 1 to Tab 4 the starting points are the solution obtained by DE.

The optimal results obtained through the optimization procedure Weighting Objectives Method, Eq. (23), are showed in Tab. 1. Observing this table one can be noted that the best solution depends on interest of the designer because each objective function is conflicting with other. In this example, when was adopted the weighting coefficients equal to 0.8 for the volume (w_1) or for the stiffness (w_3) it is obtained similar results. This is due to the fact that both are maximized and presented the similar behavior. But given the weighting coefficients equal to 0.8 for the condition number (w_2) it is observed that was obtained a different result and the dexterity was significantly improved**.** The results

indicate that this problem is very sensitive to the dexterity value. When this function is prioritized, the optimal volume and stiffness are strongly modified.

Table 2 shows the optimal results obtained by using the Global Criterion Method, Eqs. (24) and (25). In this technique the idea is to minimize the relative error of functions in relation to ideal values. The solutions obtained represent a compromise between the three objective functions. Note that the optimal is similar to the values obtained with previous method when $w_1 = 0.8$ or $w_3 = 0.8$ were chosen.

Table 1. Optimal results obtained with the Weighting Objectives Method for Example 1.

Weighting coefficients w_i	Technique	d_3 d_4 r_2 (u.l.)	Volume (u.v.)	Cond(J)	Stiffness (u.s)	Time (min)
w_1=0.33	DE	0.39 0.39 0.10	12.26	1.523	3.91	32.00
w_2=0.33	GA	0.38 0.38 0.10	11.84	1.519	3.83	91.59
w_3=0.33	SQP	0.37 0.37 0.10	11.28	1.527	3.73	1.07
w_1=0.80	DE	0.96 0.76 0.10	60.19	2.104	10.91	31.55
w_2=0.10	GA	0.98 0.72 0.10	58.13	2.023	10.65	81.34
w_3=0.10	SQP	0.97 0.73 0.10	58.99	2.057	10.77	7.00
w_1=0.10	DE	0.38 0.38 0.10	11.79	1.518	3.82	33.49
w_2=0.80	GA	0.37 0.37 0.10	11.07	1.523	3.69	74.95
w_3=0.10	SQP	0.38 0.38 0.10	11.78	1.519	3.82	4.10
w_1=0.10	DE	0.95 0.77 0.10	60.42	2.119	10.94	33.13
w_2=0.10	GA	0.96 0.76 0.10	60.01	2.097	10.89	70.01
w_3=0.80	SQP	0.95 0.77 0.10	60.43	2.120	10.94	0.91

Table 2. Optimal results obtained with the Global Criterion Method for Example 1.

	Technique	d_3 d_4 r_2 (u.l.)	Volume (u.v.)	Cond(J)	Stiffness (u.s)	Time (min)
L_{2r}-metric	DE	0.98 0.70 0.10	57.43	2.003	10.57	41.72
	GA	0.94 0.68 0.20	53.53	2.004	9.91	84.44
	SQP	0.98 0.71 0.10	57.44	2.004	10.57	3.41
L_{3r}-metric	DE	0.96 0.75 0.10	59.54	2.076	10.83	41.52
	GA	0.98 0.71 0.11	57.81	2.016	10.58	81.45
	SQP	0.97 0.74 0.10	59.27	2.068	10.80	1.22

Observing the Tab. 1 and Tab. 2 it appears that the sequential and random techniques obtained similar values, differing only in the computational cost. In the case of SQP, the results were good because the initial estimate is the optimal obtained by DE. Using sequential programming, the computational cost was significantly small, but this technique has some limitations, for example: if the model is multimodal, it can "get stuck" in some local solutions; it only handles real variables; the objective function and the constraints must both be continuous.

Considering the L_{2r}-metric, the optimal point obtained by Differential Evolution is marked in Fig. 5a). The optimal cross section area of the workspace is presented in Fig. 5b). Comparing the radial section of Fig. 5b) to Fig. 3a), one can observe that the project parameters result in a manipulator with a bigger volume (the void of the workspace was reduced). The optimal manipulator belonging to the topology WT_1 ($d_2 = 1$, $r_3 = 0$) is represented in Fig. 5c).

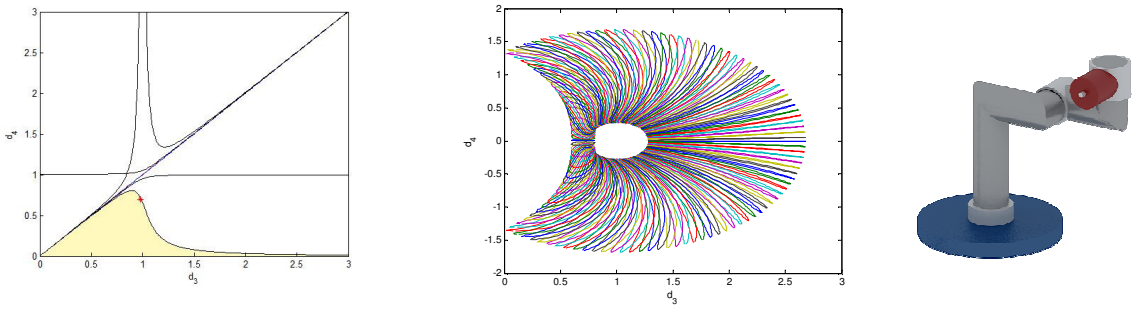

(a) Parameters space with $d_2 = 1$, $r_3 = 0$ (b) Cross section area of the workspace (c) Scheme for 3R Robot

Figure 5. The optimum design of a 3R Robot, considering the L_{2r}-metric by Differential Evolution – Example 1

5.2 Example 2 – WT_3(4, 0)

Now, considering that designer desires a manipulator that belongs to the topology WT_3, the following constraints are adopted:

Side limits: $0.1 < d_3 < 3.0$; $0.1 < d_4 < 3.0$ e $0.1 < r_2 < 3.0$ [u.l.]; (27)
Points above the curve E_1, given by Eq. (6) and Points below the curve E_2, given by Eq. (7).

The ideal solution calculated using DE is: V_{id} =1896.784 [u.v.]; $Cond(J)_{id}$ =1.317 and S_{id} =94.000 [u.s.]. For this case, the optimal results obtained through the optimization procedure Weighting Objectives Method are showed in Tab. 3. The Tab. 4 shows the results obtained by using Global Criterion Method. As observed in Example 1, the best solution depends on interest of the designer.

Table 3. Optimal results obtained with the Weighting Objectives Method for Example 2.

Weighting coefficients w_i	Technique	d_3 d_4 r_2 (u.l.)	Volume (u.v.)	Cond(J)	Stiffness (u.s)	Time (min)
w_1=0.33	DE	3.00 3.00 3.00	1896.80	2.023	94.00	6.61
w_2=0.33	GA	3.00 3.00 3.00	1896.80	2.023	94.00	70.65
w_3=0.33	SQP	3.00 3.00 3.00	1896.80	2.023	94.00	0.46
w_1=0.80	DE	3.00 3.00 3.00	1896.80	2.023	94.00	54.37
w_2=0.10	GA	3.00 3.00 3.00	1896.80	2.023	94.00	73.89
w_3=0.10	SQP	3.00 3.00 3.00	1896.80	2.023	94.00	0.43
w_1=0.10	DE	3.00 1.72 3.00	1008.50	1.317	57.90	15.72
w_2=0.80	GA	3.00 1.72 3.00	1008.50	1.317	57.89	80.15
w_3=0.10	SQP	3.00 1.72 3.00	1008.10	1.317	57.88	1.66
w_1=0.10	DE	3.00 3.00 3.00	1896.80	2.023	94.00	67.21
w_2=0.10	GA	3.00 3.00 3.00	1896.80	2.023	94.00	68.67
w_3=0.80	SQP	3.00 3.00 3.00	1896.80	2.023	94.00	0.43

Considering the L_{2r}-metric, the optimal point obtained by Differential Evolution is marked in Fig. 6a). The scheme of the optimal manipulator belonging to the topology WT_3 is illustrated in Fig. 6b).

Table 4. Optimal results obtained with the Global Criterion Method for Example 2.

	Technique	d_3 d_4 r_2 (u.l.)	Volume (u.v.)	Cond(J)	Stiffness (u.s)	Time (min)
L_{2r}-metric	DE	3.00 2.61 3.00	1596.47	1.865	81.89	19.20
	GA	3.00 2.61 3.00	1596.50	1.865	81.89	90.69
	SQP	3.00 2.61 3.00	1596.50	1.865	81.89	2.38
L_{3r}-metric	DE	3.00 2.42 3.00	1458.42	1.810	76.46	21.34
	GA	3.00 2.42 3.00	1458.50	1.810	76.46	86.12
	SQP	3.00 2.42 3.00	1458.50	1.810	76.46	7.51

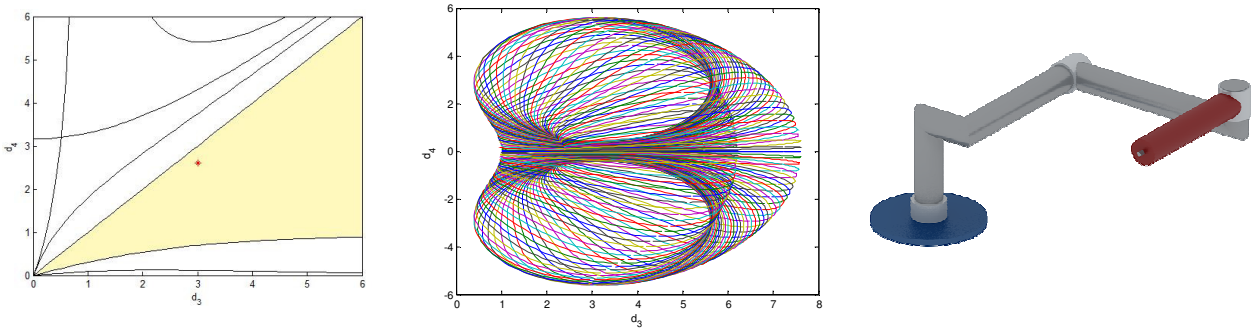

(a)Parameters space with d_2=1, r_3=0 (b) Cross section area of the workspace (c) Scheme for 3R Robot

Figure 6. The optimum design of a 3R Robot, considering the L_{2r}-metric by Differential Evolution – Example 2

The optimal cross section area of the workspace is presented in Fig. 6b). Comparing the radial section of Fig. 6b) to Fig. 3c), one can observe that the workspace is increased. Furthermore, the manipulators of this type of topology remain with 4 cusp points, a region with 4 solutions and other with 2 solutions in IKM.

Is important to note that the applied methodologies were effective to obtain an optimum which obeys the topology constraints.

5.3 Input and Output Window Program

A input data window and a output optimal results window was developed to facilitate the use of computational code, as shown in Fig. 7a) and 7b), respectively.

In the input window the designer can choose the multi-objective optimization method, the type of topology and define the side constraints. In the output window can be seen the volume, stiffness and dexterity optimal values. Moreover, it presents the optimal dimensions and the cross section area of the workspace.

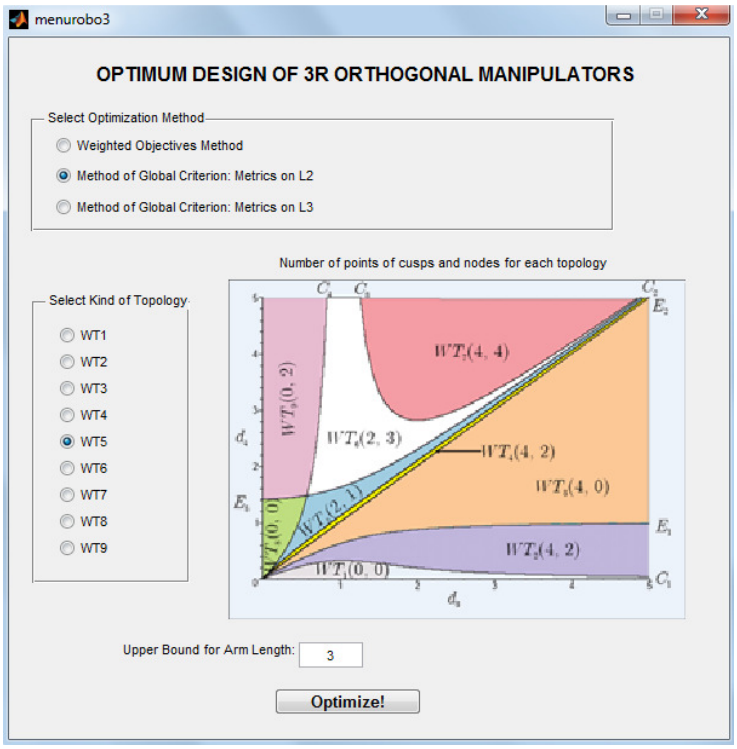

(a)

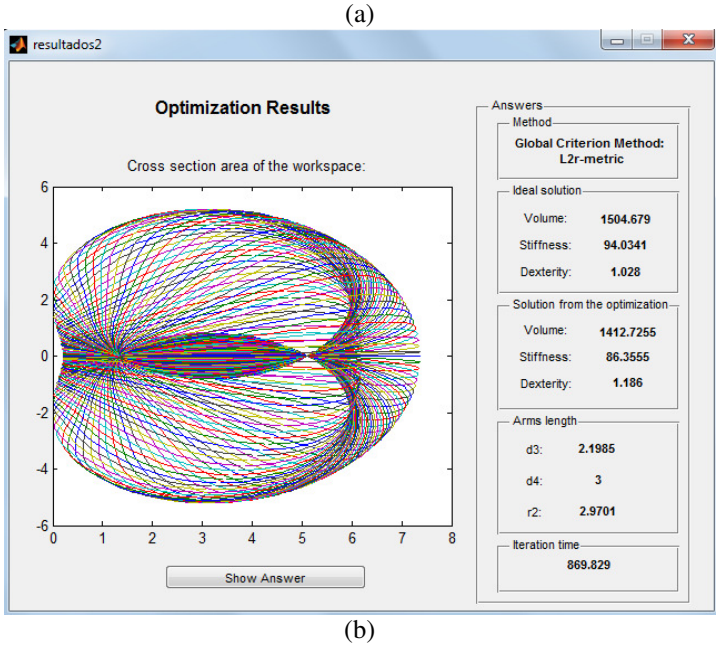

(b)

Figure 7. (a) Input data window; (b) Output optimal results window for the topology $WT_5(2,1)$, Fig.3(e)

6. CONCLUSIONS

In this work, a suitable formulation of the optimal design of manipulators with three orthogonal rotational joints was used. The aim is to obtain the optimal dimensions of the manipulators so that the maximum volume of the workspace, the maximum stiffness of the mechanism and the optimization of dexterity are considered simultaneously.

In addition, were imposed constraints according to the type of workspace topology by using appropriate equations written according to the separation surfaces of different domains. The solutions were obtained by means of two evolutionary techniques and one sequential.

The authors developed a computational code in MATLAB®, easy to be used by the designer, allowing the optimum design of manipulations can be calculated considering the most appropriate topology for the tasks.

The main contributions of this work were: to verify that the dexterity has a great influence on the optimal dimensions of the manipulators; enable the designer to choose one type of topology to obtain the best design that matches the desired application.

In the future work other examples with different topology constraints will be studied and the general case for the 3R manipulator, adopting the parameter $r_3 \neq 0$, will be considered.

7. ACKNOWLEDGEMENTS

The authors acknowledge the Fundação de Amparo a Pesquisa do Estado de Minas Gerais (FAPEMIG) by the financial support.

8. REFERENCES

Baili, M. and Wenger Ph., Chablat D., 2004, “Analise et Classification de Manipulateur 3R à axes Orthogonaux”, Thèse de Doctorat - University of Nantes, France.

Bergamaschi, P.R., Nogueira, A.C. and Saramago, S.F.P., 2006, “Design and optimization of 3R manipulators using the workspace features”, Applied Mathematics and Computation, Elsevier, Vol. 172. No.1., pp. 439-463.

Corvez, S. and Rouillier, F., 2002, “Using computer algebra tools to classify serial manipulators”, Proceeding Fourth International Workshop on Automated Deduction in Geometry, Lins.

Houck, C.R.; Joinez, J.A. and Kay, M.G., 1985, “A Genetic Algorithms for Function Optimization: a Matlab Implementation. NCSO-IE Technical Report”, University of North Caroline, USA.

Oliveira, G.T.S., Nogueira, A.C., Saramago, S.F.P., 2009, “Use of the Grobner Basis in the Study of Manipulators Topology”, Proceedings of the 20th International Congress of Mechanical Engineering, Gramado, 20th COBEM, 2009. v.1. Brazil.

Oliveira, L.S. and Saramago, S.F.P., 2010, “Multiobjective Optimization Techniques Applied to Engineering Problems”, Journal of the Brazilian Society of Mechanical Sciences and Engineering, Vol.XXXII, pp.94 - 104, 2010.

Nocedal, J., Wright, S.J., 2000, “Numerical Optimization”, Springer Series in Operations Research.

9. RESPONSIBILITY NOTICE

The authors are the only responsible for the printed material included in this paper.